Appl Nanosci (2015) 5:629–634
DOI 10.1007/s13204-014-0360-z

CrossMark

ORIGINAL ARTICLE

Electronic properties and charge control of δ-doped GaAs/$Al_{0.3}Ga_{0.7}As$ and $In_{0.53}Ga_{0.47}As$/InP core–shell nanowires

Matthew Zervos

Received: 5 June 2014 / Accepted: 12 September 2014 / Published online: 1 October 2014
© The Author(s) 2014. This article is published with open access at Springerlink.com

Abstract The electronic sub-band structure, potential profile and charge distribution of delta(δ)-doped GaAs/$Al_{0.3}Ga_{0.7}As$ and $In_{0.53}Ga_{0.47}As$/InP core–shell nanowires have been investigated in the effective mass approximation by varying systematically the position and sheet density of the δ-layer. The one-dimensional electron gas charge distribution has a maximum at the core but not at the GaAs/$Al_{0.3}Ga_{0.7}As$ or $In_{0.53}Ga_{0.47}As$/InP interfaces, as in the case of epitaxial layer heterojunctions, irrespective of the position of the δ-layer. In contrast, carriers can be confined in a quasi-triangular potential well occupying several sub-bands that fall below the Fermi level at an InP/$In_{0.53}Ga_{0.47}As$ core–shell heterojunction with a wider bandgap core, resembling the case of epitaxial layer heterojunctions, or in an InP/InGaAs/InP multiple core–shell nanowire. We discuss the need for adjusting the doping level to avoid strong band bending causing a shift of the charge distribution to the core.

Keywords Delta(δ)-Doping · III-V · Nanowires · Charge Control

Introduction

III–V compound semiconductor nanowires (NWs) with a changing composition in the axial or radial direction such as InAs/InP/InAs/InP/InAs axial NW resonant tunneling diodes (RTDs) (Björk et al. 2002) or GaAs/AlGaAs core–shell NW field effect transistors (FETs) (Morral et al. 2008; Heigoldt et al. 2009) are important for the fabrication of emerging devices in view of the ongoing downscaling of integrated circuits (ICs). In particular the ability to obtain high mobility III–V NWs on Si is important for increasing the speed of ICs as shown by (Tomioka et al. 2012) who used delta(δ)-doping to obtain a high-performance InGaAs/InP/InAlAs/InGaAs core–shell NW FET on Si. The band profile and charge distribution in this InGaAs/InP/InAlAs/InGaAs core–shell NW FET were calculated in the effective mass approximation via the self-consistent solution of the Poisson–Schrödinger equations taking into account a two-dimensional density of states applicable to quantum wells. It was shown that the charge is confined in a quasi-triangular potential well at the interface similar to the case of epitaxial heterostructures (Heigoldt et al. 2009). The ability to tailor the charge or carrier density and its spatial distribution or location is very important and may be achieved by delta(δ)-doping. In the case of a single δ-layer of n-type impurities in an epitaxial layer of GaAs electrons are confined in a *V*-shaped electrostatic potential due to the positively ionized impurities. The two-dimensional electron gas (2DEG) is confined in the vicinity of the δ-layer which may be deposited at any distance below the surface of the epitaxial layer by interrupting the growth process. Delta(δ)-doping has been used to tailor the band profile and charge distribution in AlGaAs/GaAs heterojunctions or GaAs/InGaAs/GaAs quantum wells (Ke et al. 1996; Zervos et al. 1998, 1999). However, delta(δ)-doping in III–V core–shell NWs has not been explored in great detail. Delta(δ)-doping was initially proposed by (Zhong et al. 2004) as a way to improve the carrier mobility in semiconductor NWs while the transport properties of single δ-layers of P (n-

M. Zervos
Nanostructured Materials and Devices Laboratory,
Nanotechnology Research Center, Nicosia, Cyprus

M. Zervos (✉)
Department of Mechanical and Manufacturing Engineering,
School of Engineering, University of Cyprus, P.O. Box 20 537,
Nicosia 1678, Cyprus
e-mail: zervos@ucy.ac.cy

type) or B (p-type) in Si NWs grown by the vapor–liquid–solid (VLS) mechanism were investigated by (Park 2008) who showed that δ-doping results into an increase of mobility and transconductances of NW FETs by a factor of forty. In contrast, single δ-layers in III–V NWs with a uniform composition have not been investigated in a similar way to gain an understanding of the impurity incorporation and re-distribution mechanisms and its effect on the transport properties despite the fact that δ-doping is promising for the realization of high-performance nanoscale devices according to (Lucot et al. 2011). Recently, the electronic sub-band structure and charge distribution of single δ-layers in GaAs NWs were investigated from a theoretical point of view in cylindrical coordinates and the effective mass approximation (Zervos 2013). However, there are no investigations on tailoring the electronic sub-band structure and charge distribution of III–V core–shell NWs using δ-doping which is important for the realization of optimum performance nanoelectronic devices. Hence, the electronic properties of delta(δ)-doped GaAs/$Al_{0.3}Ga_{0.7}As$ and $In_{0.53}Ga_{0.47}As$/InP core–shell NWs such as the energetic position of the one-dimensional sub-bands, corresponding wavefunctions, charge distribution and potential profile have been investigated via the self-consistent solution of the Poisson–Schrödinger equations in cylindrical coordinates and the effective mass approximation using a one-dimensional density of states and by varying systematically the position and sheet density of the δ-layer similar to the case of epitaxial layer heterostructures (Ke et al. 1996; Zervos et al. 1998, 1999). We find that the one-dimensional electron gas (1DEG) charge distribution has a maximum at the core but not at the GaAs/$Al_{0.3}Ga_{0.7}As$ or $In_{0.53}Ga_{0.47}As$/InP interface irrespective of the position of the δ-layer given since the Fermi level is pinned below the conduction band edge at the surface. However, a 1DEG can be confined in a quasi-triangular potential well occupying several sub-bands that fall below the Fermi level at an InP/$In_{0.53}Ga_{0.47}As$ core–shell heterojunction or in a square-like potential in a InP/$In_{0.53}Ga_{0.47}As$/InP core–shell NW given that the doping level is adjusted carefully to avoid strong band bending causing a shift of the charge distribution to the core.

Theory

Here we will consider the case of infinitely core–shell NWs in cylindrical coordinates so that the effective mass m^* and permittivity ε_r do not depend on $-z$ or $-\theta$. In this case, electrons are free along $-z$ but are confined in $-r$ and $-\theta$ and occupy one-dimensional sub-bands in the conduction band (CB) forming a one-dimensional electron gas (1DEG) charge distribution. To determine the energetic position of the one-dimensional sub-bands, their occupancy, overall charge distribution and band bending it is necessary to solve the Poisson–Schrödinger's equations in $-r$ and $-\theta$ in a self-consistent fashion. In such a self-consistent calculation, Schrödinger's equation is initially solved for a trial potential V and the charge distribution ρ is subsequently determined by multiplying the normalized probability density, $|\psi_k|^2$, by the thermal occupancy of each sub-band with energy E_k using Fermi–Dirac statistics and summing over all k. The Poisson equation is then solved for this charge distribution to find a new potential V' and the process is repeated until convergence is reached. Therefore, we consider first Schrödinger's equation in $-r$ and $-\theta$ which is given by,

$$-\frac{\hbar^2}{2}\left[\frac{\partial}{\partial r}\frac{1}{m^*}\frac{\partial\psi}{\partial r}+\frac{1}{r}\frac{1}{m^*}\frac{\partial\psi}{\partial r}+\frac{1}{r^2}\frac{\partial}{\partial\theta}\frac{1}{m^*}\frac{\partial\psi}{\partial\theta}\right]+V\psi=E\psi, \tag{1}$$

where $\hbar$ is Planck's constant divided by 2π, $m^*(r,\theta)$ is the effective mass of the electron, $V(r,\theta)$ is the conduction band edge potential, $\psi(r,\theta)$ is the wavefunction and E the corresponding sub-band energy. We assume that the potential is circularly symmetric and hence we consider wavefunctions of the form $\psi(r,\theta)=\psi(r)e^{im\theta}$ where $m=0,\ \pm1,\ \pm2,\ \pm3,\ldots$ is the angular momentum quantum number corresponding to quantization in $-\theta$. The potential $V(r)$ is related to the electrostatic potential $\phi(r)$ via

$$V(r)=-e\phi(r)+\Delta E_C^{i,i+1}(r), \tag{2}$$

where $\Delta E_C^{i,i+1}(r)$ is a pseudopotential due to the band offset between materials of different composition in adjacent shells i and $i+1$. Finite differences are used to express Schrödinger's equation into a standard matrix eigenvalue problem, i.e.,

$$H_m\Psi_m=E_m\Psi_m, \tag{3}$$

where H_m is the Hamiltonian matrix for a specific angular momentum number m, which is described in detail elsewhere (Zervos and Feiner 2004). To verify the correctness of the matrix setup, the ground state energy and wavefunction were calculated for a core–shell NW consisting of a 100 Å GaAs core surrounded by a 100 Å AlGaAs shell with $m^*_{AlGaAs}=0.092\ m_o$, $m^*_{GaAs}=0.067\ m_o$ and $\Delta E_C=0.23$ eV at the GaAs/AlGaAs heterointerface by solving the Schrödinger along $-r$. The step-like potential was zero everywhere inside the GaAs core and equal to $\Delta E_C=0.23$ eV in the AlGaAs shell. The lowest state $E_{n=1,m=0}=24$ meV was found to be in excellent agreement with the numerical results of Harrison (Dots 1081) derived using the shooting method. The dependence of $E_{n=1,m=0}$ on the radius of the GaAs/AlGaAs NW was also checked and found to be in agreement with Harrison (Dots 1081), i.e., for a 40 Å

GaAs/100 Å AlGaAs NW, $E_{n=1,m=0} = 96$ meV. In the case of an infinitely long nanowire, the wavefunctions take the form $\psi(r, z, \theta) = \psi(r)e^{im\theta}e^{ilz}$ and are normalized according to,

$$(2\pi)^2 \int_0^R r|\Psi(r)|^2 dr = 1, \quad (4)$$

where R is the radius of the nanowire. The one-dimensional electron gas (1DEG) density is given by the expression,

$$n_{1DEG}(r) = \sum_k n_k |\Psi_k(r)|^2, \quad (5)$$

where summation runs over the sub-bands and for each k the angular momentum quantum number takes on the values $m = 0, \pm1, \pm2, \pm3,\ldots$ Furthermore n_k is the thermal occupancy of the kth sub-band which is given by,

$$n_k = \frac{1}{\pi}\sqrt{\frac{2m^* k_B T}{\hbar^2}} \Im_{-1/2}\left(\frac{E_F - E_k}{k_B T}\right), \quad (6)$$

where k_B is Boltzmann's constant, T is the temperature, E_F is the Fermi level, E_k the energy of the bottom of the kth sub-band and $\Im_{-1/2}$ the Fermi–Dirac integral of order –1/2. The factor in front of $\Im_{-1/2}$ comes from the 1D density of states (DOS) and the units of n_k are those of a line density (m^{-1}), which when multiplied by the normalized probability density gives the volume density $n_{1DEG}(r)$. The overall charge density $\rho(r)$ is then given by,

$$\rho(r) = e(N_D^+(r) - n_{1DEG}(r)) \quad (7)$$

where e is the electron charge and $N_D^+(r)$ is the distribution of the ionized donor impurities which is assumed to be known. Using $\rho(r)$ and the potential $V(r)$ which is related to the electrostatic potential $\phi(r)$ via $V(r) = -e\phi(r)$, it is possible to solve the Poisson equation in cylindrical coordinates,

$$\frac{\partial^2\phi}{\partial r^2} + \frac{1}{r}\frac{\partial\phi}{\partial r} = -\frac{\rho(r)}{\varepsilon_o\varepsilon_r} \quad (8)$$

where ε_o is the permittivity of free space and ε_r is the relative permittivity. The exact or self-consistent potential $\phi_0(r)$ is expressed in terms of the trial potential $\phi(r)$ and a correction potential $\delta\phi(r)$,

$$\phi_o(r) = \phi(r) + \delta\phi(r) \quad (9)$$

This is substituted into Poisson's equation which is solved to find $\delta\phi(r)$. However, it is necessary to find an expression for the change in the quantum density $n_{1DEG}(r)$ given a small change $\delta\phi$. This is required since $n_{1DEG}(r)$ is also dependent on the potential ϕ, i.e., $n_{1DEG}(r,\phi)$. A perturbation $\phi \to \phi + \delta\phi$ will change the quantum electron density from $n_{1DEG}(\phi)$ to $n_{1DEG}(\phi + \delta\phi)$,

$$n_{1DEG}(\phi + \delta\phi) = n_{1DEG}(\phi) + \delta n_{1DEG}(\phi, \delta\phi) \quad (10)$$

The method of Trellakis et al. (Trellakis et al. 1997) is adopted who derives an expression for $\delta n_{1DEG}(\phi, \delta\phi)$ applicable to quantization in an infinite nanowire of square cross-section and then using the derivative property of the Fermi–Dirac integrals simplifies $n_{1DEG}(\phi + \delta\phi)$ to,

$$n_{1DEG}(\phi + \delta\phi) = \frac{1}{\pi}\sqrt{\frac{2m^* k_B T}{\hbar^2}} \sum_k \psi_k^2(\phi) \Im_{-3/2}\left(\frac{E_F - E_k + q\delta\phi}{k_B T}\right) \quad (11)$$

Using $\delta n_{1DEG}(\phi, \delta\phi)$ and $n_{1DEG}(\phi + \delta\phi)$ in Poisson's equation, yields an expression that may be expressed in matrix form and is effectively a linear system of equations in the unknown vector $\delta\phi$. After adding $\delta\phi(r, z)$ onto the trial potential $\phi(r, z)$ the process of solving the Poisson–Schrödinger equations is repeated until convergence is reached, i.e., when the average of the $\delta\phi(r, z)$ is typically less than 0.1 meV and charge neutrality is achieved which was always checked to confirm the validity of the solution.

Results and discussion

We will consider first the case of a modulation-doped (MD) core–shell GaAs/$Al_{0.3}Ga_{0.7}As$ NW to obtain an understanding of the single heterojunction and compare to the case of epitaxial layer GaAs/$Al_{0.3}Ga_{0.7}As$ heterojunctions. In this case, the GaAs and $Al_{0.3}Ga_{0.7}As$ are lattice matched and the GaAs/$Al_{0.3}Ga_{0.7}As$ heterointerface is of type I according to (; Pryor and Pistol 2005, 2008). In addition, we take into account (a) the position of the Fermi level with respect to the CB edge at the surface which is pinned at the middle of the gap (b) the dielectric permittivity $\varepsilon_R = 13.1$ and effective mass of electrons $m_e^* = 0.067\ m_o$ in GaAs (c) $\varepsilon_R = 13.1$ and $m_e^* = 0.092\ m_o$ in $Al_{0.3}Ga_{0.7}As$ and (d) the CB offset at the GaAs/$Al_{0.25}Ga_{0.75}As$ interface, i.e., $\Delta E_C \approx 0.6\ \Delta E_G = 0.25$ eV.

The CB profile of a 25-snm GaAs/20 nm $Al_{0.3}Ga_{0.7}As$/5 nm GaAs core–shell NW which is uniformly doped to 5×10^{18} cm^{-3} with Si impurities in the $Al_{0.3}Ga_{0.7}As$ shell is shown as an inset in Fig. 1a. We should note that the surface shell of GaAs which is grown to prevent oxidation of the $Al_{0.3}Ga_{0.7}As$ is depleted throughout. The CB profile has a parabolic U-like shape in the $Al_{0.3}Ga_{0.7}As$ barrier and the 1DEG charge distribution has a maximum at the core but not in the immediate vicinity of the $Al_{0.3}Ga_{0.7}As$/GaAs interface. The 1DEG charge distribution extends into the $Al_{0.3}Ga_{0.7}As$ barrier due to the high doping level and increased band bending which make the CB edge fall below the Fermi level in the vicinity of the interface. This is different to the case of epitaxial layer GaAs/AlGaAs heterojunctions, where the 1DEG charge distribution is

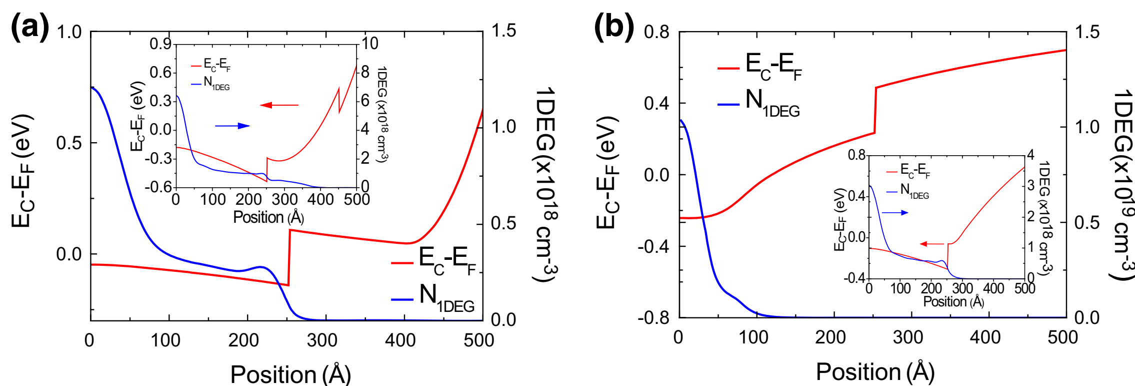

Fig. 1 CB profile and 1DEG charge distribution of a core–shell GaAs/$Al_{0.3}Ga_{0.7}As$ NW with **a** δ-layer of 10 nm with $N_{2D} = 1 \times 10^{13}$ cm^{-2} at the surface; inset shows GaAs/$Al_{0.3}Ga_{0.7}As$/GaAs core–shell NW with uniform doping of 5×10^{18} cm^{-3} in the $Al_{0.3}Ga_{0.7}As$ **b** δ-layer of 8 nm and $N_{2D} = 8 \times 10^{12}$ cm^{-2} at the core; inset shows δ-layer of 4 nm and $N_{2D} = 4 \times 10^{12}$ cm^{-2} at the GaAs/$Al_{0.3}Ga_{0.7}As$ interface

confined in a quasi-triangular potential well at the interface and is attributed to the fact that the boundary conditions are different in the case of epitaxial layer heterojunctions where the Fermi level is pinned below the conduction band edge at the surface and is also fixed with respect to the CB edge far from the GaAs/AlGaAs interface as governed by the doping level in the GaAs buffer layer. In the case of GaAs/AlGaAs NWs, the Fermi level is not fixed with respect to the CB edge at $r = 0$ but only the electric field is always zero at $r = 0$ by virtue of Gauss's law.

Delta(δ)-doping may be used to tailor the potential profile but not the concentric position of the 1DEG charge distribution. More specifically, the CB profile of a δ-doped GaAs/$Al_{0.3}Ga_{0.7}As$ core–shell NW is shown in Fig. 1a where the δ-layer at the surface has a width of 10 nm and a sheet density of 1×10^{13} cm^{-2}. In this case, three sub-bands fall below the Fermi level and the 1DEG charge distribution has a maximum at the core. Note that the CB edge on the right of the GaAs/$Al_{0.25}Ga_{0.75}As$ interface resides above the Fermi level thereby preventing the 1DEG from spreading into the $Al_{0.25}Ga_{0.75}As$ barrier which is observed in the case of uniform doping as shown in the inset of Fig. 1a. Similarly δ-doping at the GaAs/$Al_{0.25}Ga_{0.75}As$ interface, shown as an inset in Fig. 1b, resembles the energy band diagram of a GaAs/$Al_{0.25}Ga_{0.75}As$ epitaxial layer heterojunction. A total of six sub-bands are obtained when the δ-layer has a width of 4 nm and a sheet density of 4×10^{12} cm^{-2} but the 1DEG charge distribution has a maximum at the core. Finally δ-doping at the core gives two sub-bands as opposed to six for δ-doping at the GaAs/$Al_{0.25}Ga_{0.75}As$ interface but the 1DEG has again a maximum at the core as shown in Fig. 1b. In all of these cases, the carrier mobility is anticipated to be highest when the δ-layer is at the surface and is lowest when confined to the core. Evidently one may tailor the carrier density but it is difficult to control the radial position of the 1DEG and obtain confinement in the immediate vicinity of the GaAs/$Al_{0.3}Ga_{0.7}As$ heterojunction.

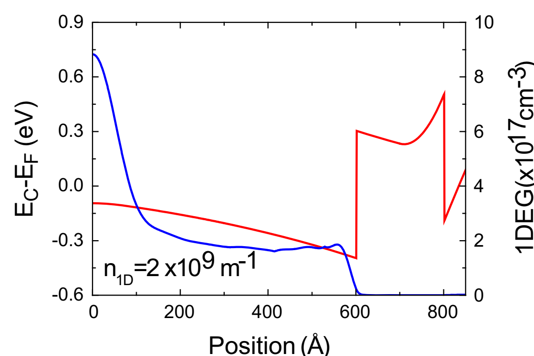

Fig. 2 CB profile and 1DEG charge distribution of an $In_{0.53}Ga_{0.47}As$/InP/$In_{0.53}Ga_{0.47}As$ NW with δ-layer of 10 nm and $N_{3D} = 1 \times 10^{18}$ cm^{-3} in the InP barrier

We observe similar trends in the case of $In_{0.53}Ga_{0.47}As$/InP/$In_{0.53}Ga_{0.47}As$ core–shell NWs. More specifically, the energy band diagram of a 600 Å $In_{0.53}Ga_{0.47}As$/200 Å InP/100 Å $In_{0.53}Ga_{0.47}As$ core–shell NW with a δ-layer having a spread of 10 nm and $N_{3D} = 5 \times 10^{18}$ cm^{-3} in the InP barrier is shown in Fig. 2. This is similar to the δ-doped InGaAs/InP/InAlAs/InGaAs core–shell NW of (Tomioka et al. 2012) and the 1DEG charge distribution has a maximum at the core but not at the $In_{0.53}Ga_{0.47}As$/InP heterojunction. We also find that the 1DEG charge distribution remains confined to the core upon reducing the core diameter and increasing the surface shell thickness keeping all else equal. In other words, only a small fraction of the 1DEG charge distribution is confined in the surface $In_{0.53}Ga_{0.47}As$ shell. This is different to the charge distribution obtained using an SCPS solver that is applicable to quantum wells.

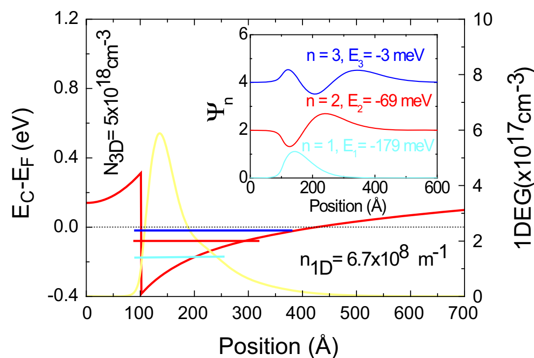

Fig. 3 CB profile and 1DEG charge distribution of an InP/$In_{0.53}Ga_{0.47}As$ core–shell heterojunction with a δ-layer of 10 nm and $N_{3D} = 5 \times 10^{18}$ cm^{-3} in the InP core; also shown the three sub-bands that fall below the Fermi level with wavefunctions confined in the quasi-triangular potential well which are offset for clarity in the inset

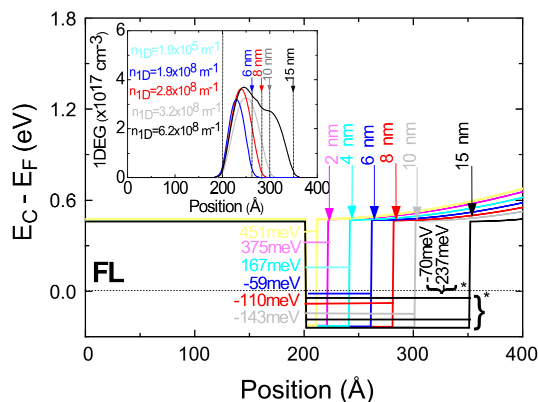

Fig. 4 CB profile of a 200 Å InP/$In_{0.53}Ga_{0.47}As$/200 Å InP with different $In_{0.53}Ga_{0.47}As$ thicknesses of 1, 2, 6, 8, 10 and 15 nm which is uniformly doped to 1×10^{18} cm^{-3} in the GaAs surface shell; inset shows 1DEG charge distributions for 6, 8, 10 and 15 nm $In_{0.53}Ga_{0.47}As$ and equivalent line densities

One may manipulate the concentric position of the 1DEG in a more effective way via the formation of an InP/$In_{0.53}Ga_{0.47}As$ core–shell heterojunction as shown in Fig. 3 where the core has a larger energy bandgap than the shell. In this case, the 1DEG is confined in a quasi-triangular potential well that extends over 200 Å and three sub-bands fall below the Fermi level while their normalized wavefunctions are shown for completeness as an inset in Fig. 3. This is very similar to the case of epitaxial layer heterojunctions and one may adjust the concentric position of the 1DEG by simply increasing the core radius but it is important to point out that there will be a slight build up of charge in the core upon increasing the doping level. Furthermore, one may attain even more control over the 1DEG charge distribution and energetic position of the one-dimensional sub-bands in an InP/$In_{0.53}Ga_{0.47}As$/InP core–shell NW. The potential profile for different $In_{0.53}Ga_{0.47}As$ shell thicknesses and a uniform distribution of $N_D = 1 \times 10^{18}$ cm^{-3} in the surface shell is shown in Fig. 4. The 1DEG is always confined in the $In_{0.53}Ga_{0.47}As$ and the potential has a parabolic-like shape in the surface shell while a flat band condition is reached in the core. More specifically, we find that a single sub-band is confined in a 10–50 Å $In_{0.53}Ga_{0.47}As$ shell but this resides energetically above the Fermi level so it is not heavily occupied and the core–shell NW is depleted throughout. However, for a 60 Å $In_{0.53}Ga_{0.47}As$ shell, we find that a single sub-band falls 59 meV below the Fermi level and the corresponding 1DEG line density is equal to 1.9×10^8 m^{-1} with a maximum of 3×10^{17} cm^{-3} keeping all else equal. This sub-band drops to 143 meV below the Fermi level upon increasing the thickness of the $In_{0.53}Ga_{0.47}As$ shell to 100 Å which is also accompanied by an increase in the 1DEG line density to 3.2×10^8 m^{-1}. In contrast, we find two sub-bands below the Fermi level when the thickness of the $In_{0.53}Ga_{0.47}As$ is 150 Å, in which case the 1DEG charge distribution is broader and has a line density of 6.2×10^8 m^{-1}. In all of these cases, the 1DEG is confined to the $In_{0.53}Ga_{0.47}As$ shell. Increasing the doping level in the InP surface shell will result into stronger band bending and a further increase in the 1DEG line density but the doping level and the surface shell thickness must be carefully controlled to prevent a shift of the 1DEG maximum to the core. The above findings are important for the design and realization of high-performance nanoelectronic devices such as core–shell NW FETs.

Conclusion

The electronic properties of delta(δ)-doped GaAs/$Al_{0.3}Ga_{0.7}As$ and $In_{0.53}Ga_{0.47}As$/InP core–shell heterojunctions, such as the energetic position of the one-dimensional sub-bands, corresponding wavefunctions and charge distribution, but also the potential profile have been investigated via the self-consistent solution of the *Poisson-Schrödinger* equations in the effective mass approximation by taking into account a one-dimensional density of states and varying systematically the position and sheet density of the δ-layer. The 1DEG charge distribution has a maximum at the core but not in the immediate vicinity of the GaAs/$Al_{0.3}Ga_{0.7}As$ or $In_{0.53}Ga_{0.47}As$/InP interfaces. In contrast a 1DEG can be confined in a quasi-triangular potential well at the InP/$In_{0.53}Ga_{0.47}As$ core–shell heterojunction with a larger band gap core, resembling the case of epitaxial layer heterojunctions or in a square-like potential in InP/$In_{0.53}Ga_{0.47}As$/InP core–shell NW but the doping level must be adjusted carefully to prevent a shift of the 1DEG charge distribution maximum to the core.

Open Access This article is distributed under the terms of the Creative Commons Attribution License which permits any use, distribution, and reproduction in any medium, provided the original author(s) and the source are credited.

References

Bertoni A, Royo M, Mahawish F, Goldoni G (2011) Electron and hole gas in modulation-doped GaAs/$Al_{1-x}Ga_xAs$ radial heterojunctions. Phys Rev B 84:205323

Björk MT, Ohlsson BJ, Thelander C, Persson AI et al (2002) Nanowire resonant tunneling diodes. Appl Phys Lett 81:4458

Harrison P, Quantum wells, Wires and Dots. ISBN 0470010819

Heigoldt M et al (2009) Long range epitaxial growth of prismatic heterostructures on the facets of catalyst-free GaAs nanowires. J Mater Chem 19:840

Ke ML, Chen X, Zervos M, Nawaz R, Elliott M (1996) Optical and electrical properties of selectively δ-doped strained $In_XGa_{1-x}As$/GaAs quantum wells. J. Appl Phy 79:2627

Lucot D, Jabeen F, Harmand JC, Patriarche G, Giraud R (2011) Quasi one-dimensional transport in single GaAs/AlGaAs core-shell nanowires. Appl Phys Lett 98:142114

Morral AFT et al (2008) Prismatic quantum heterostructures synthesized on molecular-beam epitaxy GaAs. Small 4:899

Park W (2008) Electrical Properties of Delta-Doped Silicon-Nanowire Field-Effect Transistors. J. Kor Phys Soc 53:1759

Pistol ME, Pryor CE (2008) Band structure of core-shell semiconductor nanowires. Phys Rev B 78:115319

Pryor CE, Pistol ME (2005) Band-edge diagrams for strained III–V semiconductor quantum wells, wires, and dots. Phys Rev B 72:205311

Tomioka K, Yoshimura M, Fukui T (2012) A III–V nanowire channel on silicon for high-performance vertical transistors. Nature 488:189

Trellakis A, Galick AT, Pacelli A, Ravaioli U (1997) Iteration scheme for the solution of the two-dimensional Schrödinger-Poisson equations in quantum structures. J Appl Phys 81:7880

Zervos M (2013) Delta-doping of semiconductor nanowires. Phys Stat Sol Rapid Res Lett 7:651

Zervos M, Feiner LF (2004) Electronic structure of piezoelectric InAs/InP/InAs/InP/InAs (111) nanowires. J Appl Phys 95:1

Zervos M, Bryant A, Elliott M, Beck M, Ilegems M (1998) Magnetotransport of δ-doped $In_{0.53}Ga_{0.47}As$ on InP(001) grown between 390C-575C by molecular beam epitaxy. Appl Phys Lett 72:2601

Zervos M, Westwood DI, Elliott M (1999) Light induced mobility enhancement in δ-doped GaAs/$In_{0.25}Ga_{0.75}As$/GaAs quantum wells grown by molecular beam epitaxy on GaAs(001). Appl Phys Lett 74:2026

Zhong J, Stocks GM (2004) Delta doping of semiconductor nanowires. 27th Int Conf Phys Semicond